2013

Investigation Of Leucine And Glutamic Acid Properties From The Nanoscale To The Macroscale

Thuong Ngoc Phan
Bucknell University, tnp002@bucknell.edu

Recommended Citation

Phan, Thuong Ngoc, "Investigation Of Leucine And Glutamic Acid Properties From The Nanoscale To The Macroscale" (2013). *Honors Theses*. 167.
https://digitalcommons.bucknell.edu/honors_theses/167

INVESTIGATION OF LEUCINE AND GLUTAMIC ACID PROPERTIES FROM THE NANOSCALE TO THE MACROSCALE

by

Judy Phan

Thesis Submitted to the Honors Council
For Honors in Chemical Engineering Department

04/14/2013

Approved by:

Timothy M. Raymond

Adviser: Timothy M. Raymond

Co-Adviser: Ryan Snyder

Department Chair: Jeffery Csernica

Acknowledgments

This research project would not have been possible without the support of many individuals. The author wishes to express her gratitude to her research advisor, Dr. Timothy Raymond for his support and guidance. Deepest gratitude are also due to the co-advisor, Dr. Ryan Snyder, the Honors Committee, Dr. Thomas Selby and Dr. Erin Jablonski, and the Director of Chemical Engineering Laboratories, Diane Hall. The author would also like to convey thanks to Dabrina Dutcher, the Engineering Lab Machinist, Tim Baker, Dr. Nate Siegel and Andy Hritz without their knowledge and assistance, this study would not have been successful.

Special thanks to Alexandria Hammond and James Creeley for sharing their findings of the hygroscopicity and SEM images of the studied compounds.

The author wishes to express her love and deepest gratitude to her family, friends and particularly her boyfriend for proofreading the paper and providing useful suggestions and comments.

Table of Contents

List of Tables

List of Figures

Abstract

Aerosols are known to have important effects on climate, the atmosphere, and human health. The extent of those effects is unknown and largely depend on the interaction of aerosols with water in the atmosphere. Ambient aerosols are complex mixtures of both inorganic and organic compounds. The cloud condensation nuclei (CCN) activities, hygroscopic behavior and particle morphology of a monocarboxylic amino acid (leucine) and a dicarboxylic amino acid (glutamic acid) were investigated. Activation diameters at various supersaturation conditions were experimentally determined and compared with Köhler theoretical values. The theory accounts for both surface tension and the limited solubility of organic compounds. It was discovered that glutamic acid aerosols readily took on water both when relative humidity was less than 100% and when the supersaturation condition was reached, while leucine did not show any water activation at those conditions. Moreover, the study also suggests that Köhler theory describes CCN activity of organic compounds well when only surface tension of the compound is taken into account and complete solubility is assumed. Single parameter κ was also computed using both CCN data and hygroscopic growth factor (GF). The results of κ range from 0.17 to 0.53 using CCN data and 0.09 to 0.2 using GFs. Finally, the study suggests that during the water-evaporation/particle-nucleation process, crystallization from solution droplets takes place at different locations: for glutamic acid at the particles' center and leucine at the particles' boundary.

Introduction

Aerosols are a collection liquid or solid particles that are suspended in air. Atmospheric aerosol particles are originated from either natural sources or anthropogenic sources ranging from less than 1 µm in radius (fine particles) to 10 µm in radius (coarse particles) [Jacob, 1999]. Natural atmospheric aerosols are directly emitted from volcanic eruptions, mineral dust, sea salt and biological materials (plant fragments, microorganism, pollen, etc.) [Pöschl, 2005]. Anthropogenic aerosols, on the other hand, are emitted from sources such as biomass burning, incomplete combustion of fossil fuels, traffic-related suspension of road and other dusts [Pöschl, 2005].

Aerosols are known to have various effects on climate, atmosphere, and human health. In the troposphere, aerosols have both direct and indirect influence on the Earth's climate. Reflecting or absorbing solar radiation, atmospheric aerosols directly cause the surrounding air to cool down or heat up. Indirectly, aerosols act as cloud condensation nuclei (CCN) which in turn become cloud droplets. Once formed, clouds can have a tremendous effect on the Earth's radiation budget through their albedo [IPCC, 1995]. Overall, atmospheric aerosols are thought to have a cooling effect on the global climate as opposed to greenhouse gases [Seinfeld et al., 2006; Hartmann and Doelling, 1991]. In the future, when global warming predicts a warmer and moister climate, this effect of atmospheric aerosols will become more significant [Aalto and Kulmala, 2000]. Moreover, cardiovascular, respiratory, and allergenic diseases are known to be caused by atmospheric aerosols [Pöschl, 2005]. The effects of aerosols depend on the droplet size distribution [Twomey, 1977], lifetime of clouds, and the distribution of water mass in different atmospheric layers [Hudson, 1992; Lohmann and Lesins, 2002].

As stated above, the effects of aerosol particles on global climate and human health are undoubtedly critical, but to what extent are still unknown. This large uncertainty is mainly due to our limited knowledge of nucleation processes and the interactions between aerosols and water. Moreover, CCN activities are characterized by chemical composition and physical properties of the particles. Atmospheric aerosol composition includes both inorganic and organic species. Organic species can contribute 20-50% of the fine aerosol mass as in the form of complex mixtures [Masclet and Hoyau, 1995; Saxena and Hildemann, 1996; Andrews et al, 1997]. In a recent paper, organic particulate matter can represent up to 80% of total aerosol mass [Jacobson et al., 200]. Moreover, approximately 80% of the wet-season aerosol mass in the Amazon Basin was found to be organic aerosols [Artaxo and Hansson, 1995; Wouters et al., 1993]. Another field study indicates that 63% of the CCN number-concentration measured at a marine site was organic aerosols [Novakov and Penner, 1993]. However, recent studies show that the activation capability of organic aerosols is comparable to that of sulfate aerosols, which are known to be the most effective CCN [Matsumoto et al., 1997; Acker et al., 2002]. The behavior of inorganic species is well understood [Köhler, 1936; Pruppacher and Klett, 1980; Cruz and Pandis, 1997], but CCN activation of organic particles has not been well studied. The reason is that organic aerosols' solubility in water is limited which makes them less CCN active. However, several studies have shown that organic species can still be good sources of CCN [Cruz and Pandis, 1997; Corrigan and Novakov, 1999; Raymond and Pandis, 2002; Broekhuizen et al, 2004; Sun and Ariya, 2006]. Therefore, organic species should not be neglected in studying CCN activities and the links between aerosols, clouds and climate.

The most well-known theory that predicts the activation of CCN of inorganic species is Köhler theory [1936]. The theory is based on the thermodynamic balance of the Raoult and Kelvin effects on the vapor pressure of water over a solution droplet. The Raoult effect is the decrease in vapor pressure due to the change in water activity because of the solute. The Kelvin effect is the increase in vapor pressure due to the curvature of the droplet surface. Köhler theory assumes that the chemical substance is completely soluble in water, does not have a considerable vapor pressure and has a constant mass during droplet growth. The assumptions make Köhler theory work well for inorganic species but not so much for organic species [Raymond and Pandis, 2002]. Various studies have proposed modified Köhler equations that take into account solubility, contact angle and surface tension [Shulman et al., 1996; Gorbunov and Hamilton, 1997; Laaksonen et al., 1998; Raymond and Pandis, 2002; Hori et al., 2003; Kumar et al., 2003]. While there are many theories that were developed to describe the CCN activation of organic species, there are very little experimental work that has been done to verify their results. The focus of this study is to expand the knowledge of CCN activation of pure organic compounds, particularly amino acids, and to compare the experimental results with the results of Köhler theory.

Two amino acids were chosen for this study: a monocarboxylic acid, leucine ($C_6H_{13}NO_2$), and a dicarboxylic acid, glutamic acid ($C_5H_9NO_4$) (Figure 1 and 2 respectively).

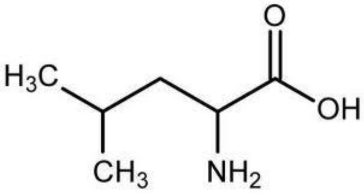

Figure 1. Molecular structure of leucine

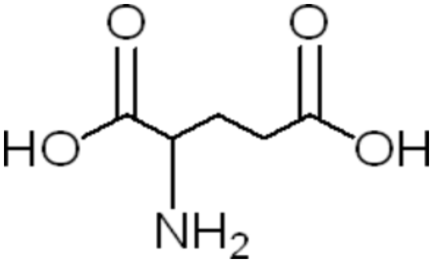

Figure 2. Molecular structure of glutamic acid

Recent studies suggest that 20-80% of total nitrogen is bound in organic compounds [Zhang et al., 2002; Mace et al., 2003; Ge et al., 2010]. In fact, amino acids (AA) contribute the most to the atmospheric organic compounds [Ge et al., 2010; Castro et al., 2001; Dennis et al., 2007; Milne et al., 1993]. AA aerosols contribute in forming secondary organic aerosols and potentially affect the radiation balance [Chan et al., 2005; de Haan et al., 2009]. Three types of AA are dissolved combined AA (DCAA, e.g. protein and peptides), dissolved free AA (DFAA, e.g. hydrolysis of DCAA), and particulate AA (PAA, e.g. µm sized solid microorganism and debris particles) [Kristensson et al., 2009]. Those AA aerosols are classified into marine and continental particles. Marine particles are emitted from bursting bubbles on surface layers of oceans [Wedyan et al., 2008; Mopper et al., 1987; Kuznetsova et al., 2005]. Continental particles are thought to come from the suspension of bacteria, yeast, fungi, algae, pollen, spores [Tong and Lighthart, 2000;

Scheller, 2001; Sattler et al., 2001; Yu et al., 2002] and biomass burning [Mace et al., 2003; Laskin et al., 2009]. Leucine and glutamic acid are found to have both the marine and continental characters [Kristensson et al., 2009]. Concentration of marine character aerosols is 130-2000 pmol of total organic mass of DFAA + DCAA + PAA m^{-3} [Wedyan and Preston, 2008]. Another study gives the concentration of DFAA from a mixed of marine and continental sources to be 1.5-220 pmol N m^{-3} [Mace et al., 2003; Matsumoto and Uematsu, 2005]. For aerosols that have continental character, their concentration is from 20-1120 pmol DFAA n m^{-3} [Mace et al. 2003].

Background Information

1. *Köhler theory:*

The CCN activity of an aerosol particle is most commonly described by Köhler theory. As introduced above, Köhler theory takes into account Kelvin and Raoult effects on the water vapor pressure over a solution droplet. The equation [Seinfeld and Pandis, 1998; Raymond and Pandis, 2002] can be written as:

$$S = \gamma_w \frac{n_w}{n_w + \frac{\pi \nu \varepsilon d_s^3 \rho_s}{6M_s}} \exp\left[\frac{4M_w \sigma_{sol}}{RTD_p \rho_{sol}}\right] \tag{1}$$

with

$$n_w = \frac{\pi\left(D_p^3 - d_s^3\right)\rho_w}{6M_w} \tag{2}$$

where

S = vapor saturation of water relative to a flat surface of pure water required for droplet equilibrium

γ_w = water activity coefficient which is assumed to be 1 because the solution is mostly water

n_w = number of moles of water in the droplet

ν = van’t Hoff factor, average number of ions that the solute molecule dissociates, assumed to be 1

d_s = dry solute particle diameter

ρ_s = density of solute

M_s = molecular weight of solute

M_w = molecular weight of water

σ_{sol} = surface tension between air and the solution

R = gas constant

T = temperature

D_p = droplet diameter

ρ_{sol} = density of solution and describe in equation (4)

ρ_w = density of water

ε = dissolved mass fraction of the solute particle and can be calculated as below

$$\varepsilon = \frac{C_{sat}\left(D_p^3 - d_s^3\right)\rho_w}{d_s^3\ \rho_s} \tag{3}$$

where

C_{sat} = solubility of the solute in water (mass per volume)

Assuming additive behavior, the density of the solution is calculated as:

$$\rho_{sol} = \frac{\varepsilon d_s^3 \rho_s + \left(D_p^3 - d_s^3\right)\rho_w}{D_p^3 - (1-\varepsilon) d_s^3} \tag{4}$$

The modified Köhler equation after substituting and simplifying is:

$$S = \frac{\gamma_w \left(D_p^3 - d_s^3\right) M_s \rho_w}{D_p^3 M_s \rho_w + d_s^3 (\varepsilon \nu M_w \rho_s - M_s \rho_w)} \exp\left[\frac{4 M_w \sigma_{sol}}{R T D_p \rho_{sol}}\right] \tag{5}$$

When ε is equal to unity, the equation can be simplified to:

$$S = \frac{\gamma_w M_s}{M_s + \nu C_{sat} M_w} \exp\left[\frac{4 M_w \sigma_{sol}}{R T D_p \rho_{sol}}\right] \tag{6}$$

These modified Köhler equations take into account the solubility and surface tension of the solute while the classical Köhler equation does not. Those factors are important when analyzing the CCN activity of less soluble compounds. Their limited solubility causes gradual dissolution in the growing droplet and also lowering the droplet surface tension [Shulman et al., 1996].

Cruz and Pandis (1997) developed another version of the Köhler equation by performing Taylor series expansion on the exponential. The equation results in an equilibrium curve for a given mass of the solute. The most important point in this curve is the maximum point where a transition state from a stable to an unstable region occurs. The corresponding supersaturation and droplet radius of this maximum point are called the critical supersaturation (S_c) and the critical radius (r_c) respectively. At a condition where the supersaturation and the droplet radii are less than S_c and r_c, the solution is in equilibrium with the environment. On the other hand, if the environment condition passes this critical point, then the solution droplets are activated and grow into cloud droplets limited only by the amount of water vapor above the solution. The critical values can be calculated as:

$$S_c = \sqrt{\frac{4A^3}{27B}} \tag{7}$$

$$r_c = \sqrt{\frac{3B}{A}} \tag{8}$$

where

$$A = \frac{4\sigma_{sol} M_w}{RT\rho_w} \text{ and } B = \frac{3\nu m_s M_w}{4\pi M_s\, \rho_w} \qquad \text{(9) and (10)}$$

From equation (9), given a supersaturation, one can calculate the minimum solute mass necessary for the nucleus to activate into a droplet. The activation or dry particle diameter can then be determined based on this solute mass and compared to experimental values.

2. *Hygroscopicity:*

As stated above, atmospheric aerosols affect the climate both directly and indirectly. Directly, atmospheric aerosols interact with the sun radiation and indirectly, they act as CCN which affects cloud properties. The magnitude of these effects, in fact, strongly depends on their interaction with water. Even when the relative humidity (RH) is less than 100%, aerosols still take on water and grow into droplets. Hygroscopicity describes the ability of particles to absorb water at a given RH with a given initial dry diameter. Hygroscopic properties of aerosols depend on two factors: the ability of the solution droplet to lower the water activity, and their influence on surface tension (Ruehl et al., 2010). A common technique that is used to measure the hygroscopicity of a specific compound is hygroscopic tandem differential mobility analyzer (HTDMA). Through this technique, hygroscopic growth factor (GF) is measured along with the changes in particles size and phases. The GF can be expressed as:

$$GF = \frac{D_p(RH)}{d_s(RH)} \tag{11}$$

In the above equation, $D_p(RH)$ is the wet particle diameter at a given higher RH compared to $d_s(RH)$ which is the dry particle diameter at a set lower RH so that a GF=1 implies no water uptake. At a phase transition RH, called deliquescence RH (DRH), the solid particle abruptly deliquesces and forms a saturated solution droplet (Gysel et al., 2002). In other words, the particles remain the same phase until this DRH is reached. Recent studies show that hygroscopic properties are particle size dependent (Biskos et al., 2006; Park et al., 2009; Russel et al., 2002) and ambient RH dependent (Hu et al., 2010). For example, when RH is below the DRH, GFs of salt aerosols decrease while dry particle diameter increases (Hu et al., 2010). When RH reaches the DRH, GFs increase with dry particle diameter (Hu et al., 2010). Large particles are easier to uptake water than smaller particles, but only when there is enough water vapor. Hu et al. (2010) also concludes that there are two regimes of effects: RH dominant regime (below DRH) where GFs increase with RH and particle size dominant (above DRH) where GFs are more sensitive to particle size.

While there are many studies on the hygroscopicity of inorganic aerosols, there is very limited information on the water interaction of organic aerosols. Posfai et al. (1998) concluded that organic aerosols were responsible for water uptake of ammonium sulfate at low RH. Another study included that film coatings of several organic species delayed the hygroscopic growth of sulfuric acid aerosol in the first few seconds (Xiong et al., 1998). These two results are contradicting with each other, so more studies are needed to understand the hygroscopic growth of organic aerosols.

3. *Kappa Parameter:*

In literature, a common parameter, called Kappa (κ) is used to characterize the relative hygroscopicity and the CCN activity of aerosols. Kappa parameter (Petters and Kreidenweis, 2007) is defined as:

$$\frac{1}{a_w} = 1 + \kappa \frac{V_s}{V_w} \tag{12}$$

The parameter relates the water activity (a_w) to the ratio of the volume of solute (V_s) to volume of water (V_w). It can be combined with Kohler theory to describe the relationship between the particle dry diameter and their CCN activity (Petters and Kreidenweis, 2007). Secondly, it can be derived from hygroscopic growth factor data that are obtained from the HTDMA to describe the ability of particles uptake water when RH is less than 100%. Parameter κ ranges from zero to 1.4, but typical particles in the atmosphere have values ranging from 0.1 to 0.9 (Petters and Kreidenweis, 2007). A high value of κ means that the particles are very soluble, highly CCN active and zero κ means that the particle is nonhygroscopic but wettable, this is when the Kohler equation is reduced to the Kelvin equation. Inorganic species such as NaCl have a high κ value ranging between 0.5 and 1.4 while organic species have a lower κ value ranging from 0.01 to 0.5.

To characterize CCN activity of a selected chemical, its CCNC data, particularly critical supersaturation and dry diameter, are fitted against known κ lines (Figure 3) to determine its κ value. Those κ values are calculated based on κ- Köhler equation (Petters and Kreidenweis, 2007):

$$S = \frac{D_p^3 - d_s^3}{D_p^3 - d_s^3(1-\kappa)} \exp\left[\frac{4M_w\sigma_{sol}}{RTD_p\rho_{sol}}\right] \tag{13}$$

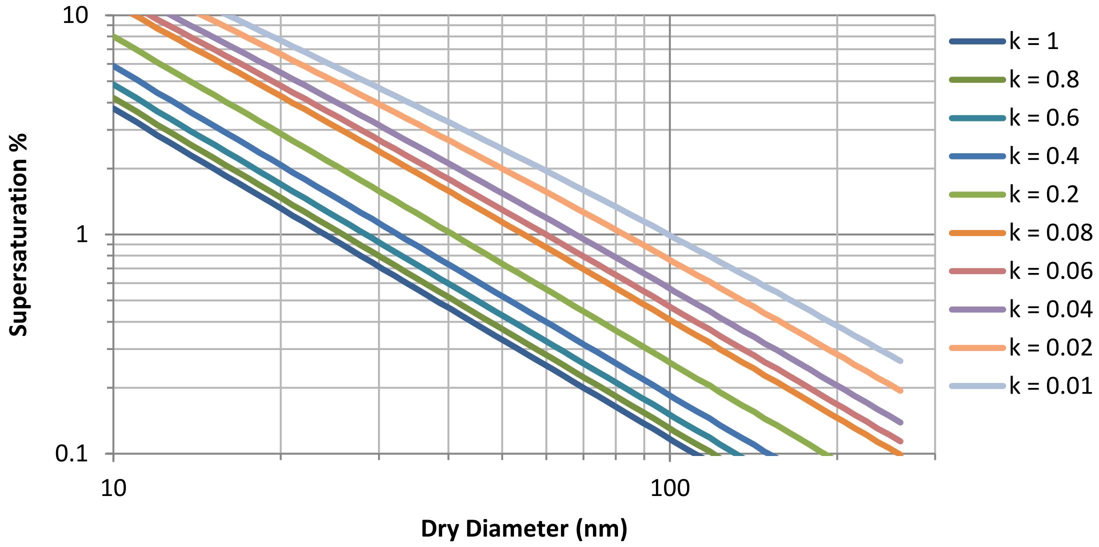

Figure 3. Constant κ values calculated for different supersaturation vs dry diameter

When obtaining κ values from the growth factors using the HTDMA method, the following equation (Petters and Kreidenweis, 2007) is used:

$$\frac{RH}{\exp\left(\frac{2A}{d_S GF}\right)} = \frac{GF^3-1}{GF^3-(1-\kappa)} \tag{14}$$

where

RH is expressed as a fraction and A is defined as shown in equation (9).

The difference between equation (14) and the κ- Köhler equation is that the wet and dry volumes are valued in HTDMA as opposed to mass or moles of the solute which were calculated using the molecular weight of density of the bulk solution (Petters and Kreidenweis, 2007). Petters and Kreidenweis paper also shows that the κ values derived from this method are within 30% agreement with the ones obtained from the CCN activity. Note that Petters and Kreidenweis assumed the solubility of all solutes to be 0.072 J m^{-2} and κ values were calculated at 298.15 K in all cases.

Experimental

1. *Solubility Tests:*

Leucine and glutamic acid were tested for their solubility at room temperature (22 °C) and standard atmospheric pressure. Initially, the literature values which are 22.4 g/L and 8.64 g/L for leucine and glutamic acid respectively were used [Mo et al., 2011; Raymond and Pandis, 2002]. The solutions were placed on a shaker for couple days, but there was still a small amount of insoluble materials left in the beaker. An additional 20 mL and 10 mL of DI water were added to the leucine and glutamic acid solutions respectively. An hour later, the solutions were clear indicating that all of the materials were completely dissolved.

2. *Pendant DropTechnique:*

Surface tension describes how strong the molecules of a liquid attract to each other at the surface. Liquids such as water have strong interactions between the surface molecules therefore have a high surface tension value and vice versa. In this study, surface tensions of leucine and glutamic acid were measured by a KSV CAM 200 Optical Contact Angle Meter. The instrument uses a technique called the pendant drop technique to measure surface tension.

Liquid drops from each solution (at their solubility limits) were drawn from a syringe and hung in the air. The instrument captured the images of these drops and relate the drop shape to surface tension through the equation (KSV CAM 200 Instruction Manual, 2001):

$$\sigma = \Delta\rho g R_0^2/\beta \tag{15}$$

where

σ = surface tension (mN/m)

$\Delta\rho$ = difference in density between air and solution

g = gravitational constant

R_0 = radius of drop curvature at apex

β = shape factor which is defined by Young-Laplace equation expressed in 3 dimensionless equations (see the manual) and can be estimated using iteration.

Given the densities of air and the liquid solution, one can determine the surface tension using this technique. The instrument has an accuracy of ±0.1mN/m.

3. *Scanning Mobility CCN Activity:*

The experimental setup is shown in Figure 4. The apparatus includes an aerosol atomizer (Constant Output Atomizer 3076, Thermo Systems Inc. (TSI)), a diffusion dryer, a neutralizer

(Aerosol Neutralizer 3077, TSI), and a Scanning Mobility Particle Sizing system (SMPS) (SMPS 3934, TSI) which consists of a differential mobility analyzer (DMA) (3071A, TSI), a Condensation Particle Counter (CPC) (CPC 3010, TSI), and a Cloud Condensation Nucleus Counter (CCNC) (CCNC-100 Droplet Measurement Technologies). The SMPS system connects to a computer to control both the scanning and counting particles.

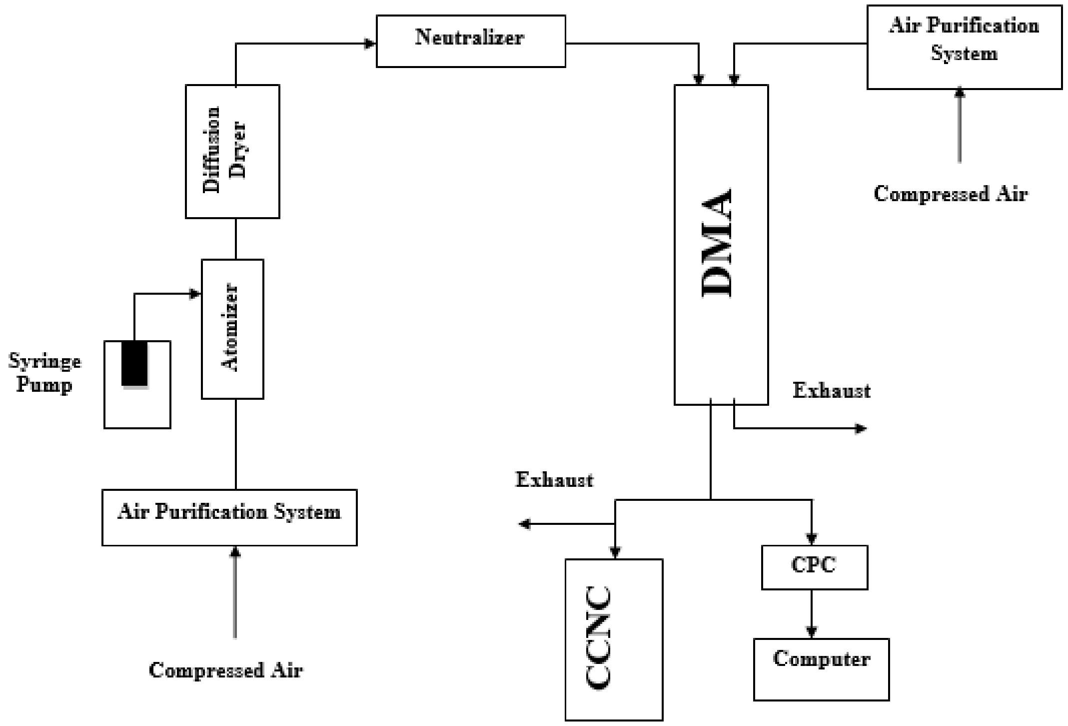

Figure 4. Schematic of experimental setup for CCN measurements

The above setup allows the user to have control over the particles size, the chemical composition of the particles and the supersaturation in the CCNC. Moreover, this setup measures and reports to the control computer the particle size, the total number concentration and the CCN concentration instantaneously. Two computer software packages are used along with the setup:

the TSI Aerosol Instrument Manager (AIM) software and the Scanning Mobility CCN Analysis (SMCA). The AIM control software scans the voltage that is applied to the DMA and manages the data obtained from the CPC to provide distribution and size of the aerosols and the raw CN counted every 0.1 seconds. The SMCA software uses the data from the SMPS to measure CCN distributions and activated droplet size as a function of mobility size over the timescale of an SMPS scan [Moore et al., 2010].

a) Monodisperse aerosol generation system

The experiment uses a collision atomizer that produces monodisperse particles of a known size of the investigated species (leucine and glutamic acid). Both solutions are made with the concentration of 1g of the investigated compound per liter of double deionized filtered water to ensure minimum impurities. The atomizer uses a high velocity air jet to provide a constant output. Filtered air is introduced into the stream to generate droplets. Then, the solution stream enters a silica gel diffusion dryer to evaporate the solvent. At this stage, the particles exit with a smaller size and are dry. This wide size of distribution of polydisperse particles then charged in a Kr-86 bipolar aerosol neutralizer. In this neutralizer, the particles achieve a nearly Boltzmann equilibrium distribution of charges [Wiedensohler, 1988]. From the neutralizer, the particles continue to travel into the DMA. By adjusting the voltage of the center rod in the DMA, desired diameters are selected according to their electrical mobility [Liu and Pui, 1974; Knutson and Whitby, 1975]. Different mean sizes of the particles exiting the DMA have nearly monodisperse distributions.

b) Aerosol classifier and total number concentration counter

The stream of monodisperse particles is split to enter the CPC and the CCNC. This CPC displays the size distribution of the particles through the control computer. The CPC uses a buffer solution of n-butanol and a laser to count the particles. As stated above, the AIM software manages the data that are sent from the CPC every 0.1 seconds during each scan.

c) CCNC

Lastly, the particles stream enters the CCNC which is a thermal gradient diffusion cloud chamber. The chamber allows flow between two vertical parallel walls. The aerosols flow along a thermal gradient, and the walls are kept wet to provide water vapor supersaturation conditions. The aerosols flow through the chamber at the top along with a stream of particle-free sheath air. When there is a difference in temperature along the walls, supersaturation condition is reached. The supersaturation inside the chamber can be adjusted from 0.1 to 2% with the maximum near the exit of the chamber by changing the temperature gradient. Particles that have the ability to become CCN (right size and chemistry) are simultaneously counted by an optical particle counter laser.

d) Experimental procedure

The setup was calibrated using NaCl and ammonium sulfate. There are two ways that this setup can be used:

- Keep the particles diameter constant and change the supersaturation percent.
- Keep the supersaturation constant and change the particles diameter.

The second procedure was used for this work to measure CCN activation curves for leucine and glutamic acid. The supersaturation was changed from 0.2 to 0.4 to 0.6 to 0.8 to 1% throughout the experiments. Each experiment was run for at least three hours to obtain sufficient data. The ratio of the concentration of activated particles to the total particle concentration (CCN/CN) was calculated.

4. Scanning Electron Microscope:

To obtain two-dimensional images of both bulk crystals and micron-sized particles of leucine and glutamic acid, a scanning electron microscope (SEM) (JEOL, JSM-6390LV) was used. Those images provide information on particle morphology including particle’s shape and surface structure. The instrument uses an electron beam and accelerates it in a low acceleration voltage region to produce high resolution images of the particles [Todokoro et al., 1999].

Samples of bulk crystals or micron-sized particles were collected on 12 mm steel disks which were covered with carbon tape. A coating of gold was also applied on the disks using a gold sputter system (Denton, Vacuum Desk IV) and Argon air. The disks were then viewed under the SEM instrument to obtain particle images.

Results and Discussion

The results and discussion are presented in five parts for leucine and glutamic acid. The investigation of solubility and surface tension will be presented first, followed by an analysis of CCN activity, then the hygroscopicity analysis, Kappa parameters, and lastly SEM images of both compounds.

1. *Solubility and surface tension:*

The first portion of this study was to verify the water solubility and surface tension of leucine and glutamic acid that are reported in the literature. Table 1 shows the water solubility results of this study as well as other studies' values. Glutamic acid has a solubility range from 6.6 to 7.2 g/L which agrees with Raymond and Pandis values [2002]. However, two other studies show a higher solubility for glutamic acid [Jin and Chao, 1992 and Mo et al., 2011]. Moreover, the result of solubility for leucine in this study is higher than what Raymond and Pandis reported [2002] but lower than the CAS database has. This demonstrates that solubility of organic compounds can have a wide range of values. Those that have optical isomers (D- vs L-) like glutamic acid and leucine possess different solubility values for each isomer.

Raymond and Pandis [2002] stated that leucine and glutamic acid have similar solubility where this study shows the opposite result. Leucine has much higher water solubility than glutamic acid (Table 1). Huff Hartz et al. [2006] also classified glutamic acid as complete solubility compound and leucine as limited solubility compound. Additionally, glutamic acid dissolves faster in water compared to leucine. This result was not expected since glutamic acid is a bigger molecule (147.13 g/mol) than leucine (131.17 g/mol). Also, glutamic acid is a dicarboxylic acid while leucine only has one acid group. Both the molecule size and the number of hydrophilic group predict that glutamic acid should have a higher solubility than leucine. The results indicate that the pH of the solutions as well as the crystal structures play an important part in obtaining the solubility of organic species.

Table 1: Solubility of leucine and glutamic acid

	Leucine [g/L]	**Glutamic Acid [g/L]**
This Study	17 - 18.7	6.6 - 7.2
Jin and Chao , 1992	NA	8.6 (l-isomer)
Raymond and Pandis, 2002	8.8 – 9.7	6.6 – 7.3
CAS DataBase	22.4	NA
Mo et al., 2011	NA	8.56

Surface tension was determined using the Pendant Drop method [Ambwani and Fort, 1979]. The samples for this test were obtained from the solution of the solubility test. Measuring surface tension of a solution that is at it saturation is important since previous study shows that only a fraction of the solute particle would dissolve at its critical activation diameter [Raymond and Pandis, 2002]. In the beginning of each test, the instrument was calibrated and water was used to test the precision of the instrument. The result showed good agreement with the literature (72.30 mN/m). Table 2 summarizes the surface tension of leucine and glutamic acid in water that was measured in this study as well as the reported literature values. Using both Young/Laplace and Bashforth/Adams fitting, the surface tension results of both compounds are higher than other studies' values. However, the two methods' results are in agreement with each other (less than ± 3 mN/m). Additionally, glutamic acid has a slightly higher surface tension than leucine (although it is the same within experimental error) which is expected since glutamic acid is slightly more hydrophilic than leucine (two acid groups vs one acid group).

Table 2: Surface tension of leucine and glutamic acid measured by Pendant Drop Method

Solution	**Literature [mN/m]**	**Young/Laplace [mN/m]**	**Bashforth/Adams [mN/m]**
Leucine (17 g/L)	70[a]	80.2 ± 3.3	82.7 ± 4.7
Glutamic Acid (6.6 g/L)	71[ab]	83.8 ± 2.6	82.8 ± 5.4

[a] Raymond and Pandis, 2002.

[b] Huff Hartz et al., 2006.

2. *CCN Activity:*

The activation diameters, D_p^{50}, at which 50% of the particles are activated, were measured for each supersaturation condition (from 0.2 to 1% SS) for glutamic acid. Leucine was not observed to activate into cloud droplets under any conditions studied. Figure 5 compares the glutamic acid experimental and theory results using Equation 7-10. One theory's result uses the assumptions that the solute is completely soluble and has the same surface tension as water. The second theory's result uses the surface tension measured by this study to calculate the activation diameters. The solubility was not taken into account since all previous studies showed that the predicted activation diameters using limited solubility were far off from the experimental results (Table 3).

All three results show that glutamic acid activates at a smaller diameter when the supersaturation is high. The experimental and theoretical results are in good agreement with each other. Köhler theory predicts slightly higher activation diameters than the experiment shows. Moreover, the theoretical results from two assumptions also show good agreement. The calculated diameters that used water properties assumption are closer to the measured values in experiment than the other one assumption. This indicates that surface tension has a significant impact on the prediction of activation diameter.

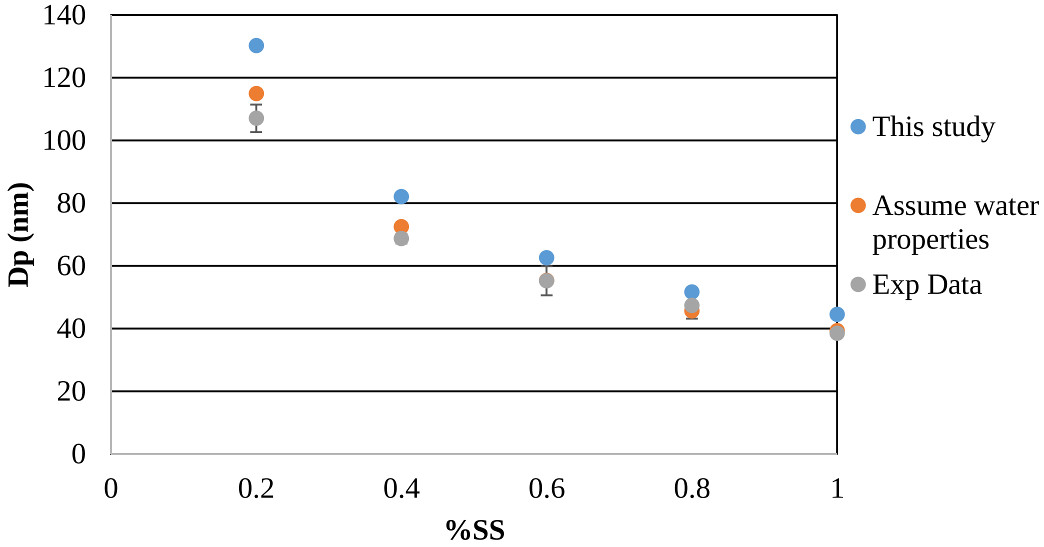

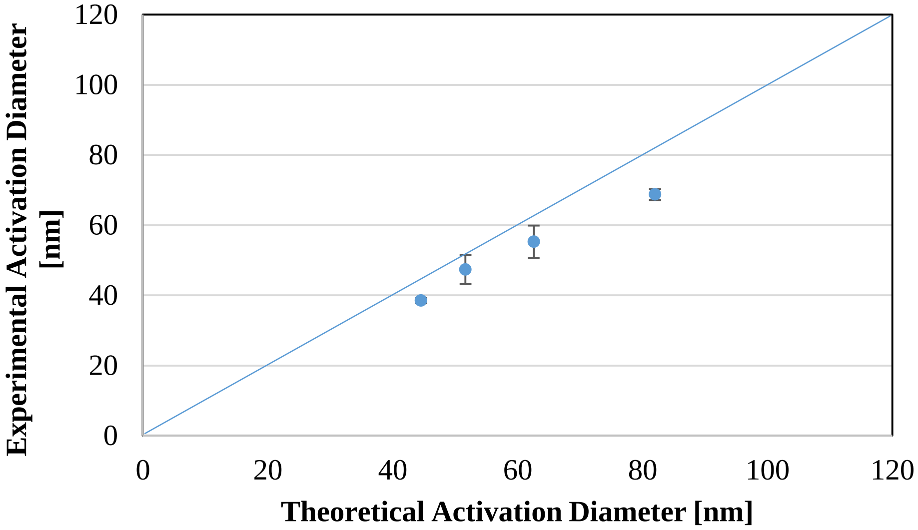

Figure 5. Comparison of CCN activity of glutamic acid. The grey markers on the top graph are experimental data using the SMCA setup as described in the Background Information section. The blue and orange markers on the bottom graph are theoretical calculations using the properties measured in this study and assuming water properties respectively.

The measured activation diameter of glutamic acid at 1% supersaturation is in good agreement with the literature values, especially with Raymond and Pandis [2002] study (Table 3). Additionally, the diameter obtained from theoretical calculation is also close to the diameters that were reported from other studies. Both Raymond and Pandis [2002] study and Huff Hartz et al. [2006] study used a lower surface tension and higher crystal density than this study. Also, Huff Hartz et al. [2006] assumed that glutamic acid has a higher solubility than leucine.

Table 3: Comparison of measured and calculated activation diameters at 1% supersaturation

	Experimental D_p^{50} [nm]	**Theoretical D_p^{50} [nm]**
This study	38.47 ± 0.74	44.53 (complete solubility)
Raymond and Pandis [2002]	38 ± 6	194 (limited solubility) 42 (complete solubility)
Huff Hartz et al. [2006]	43 ± 7 (D) 41 ± 7 (L)	189 ± 28 (limited solubility) 41 ± 6 (complete solubility)
Kristensson et al. [2010]	40 (L)	NA

Leucine did not show any activation experimentally up to 200 nm at the highest supersaturation (1%). Raymond and Pandis [2002] study also agrees with this result. On the other hand, looking at the solubility property of leucine and glutamic acid, the opposite result was predicted. Leucine has a higher solubility than glutamic acid which in theory leucine should be more CCN active than glutamic acid. Again, this observation suggests further investigation of the two species.

3. *Hygroscopicity:*

The growth by uptake of water vapor of both glutamic acid and leucine particles when RH is less than 100% was studied. Figure 6 shows the hygroscopic behavior of D_0 = 80 nm glutamic acid particles. When RH < 83% the particles remain unchanged and no particle growth was observed. At 83.3% RH, particles start taking up water and grow into bigger particles as %RH increases further. The highest size recorded was 113.4 nm which is about 1.4 times the initial diameter. This indicates that glutamic acid can activate when RH < 100% and the DRH occurs around 83.3% RH. However, there is no literature value to validate this result.

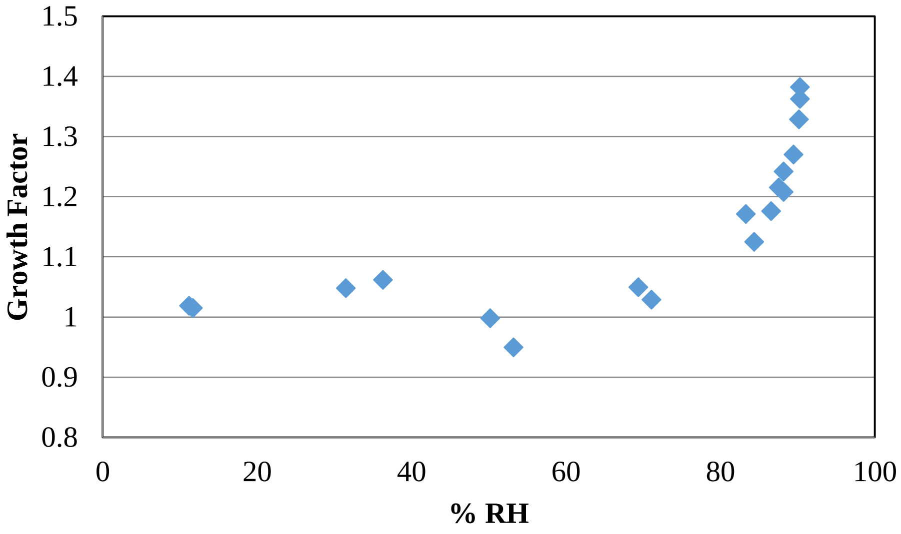

Figure 6. GF as a function of % relative humidity of glutamic acid (80nm)

The hygroscopic behavior of D_0 = 80 nm leucine particles was also investigated. In contrast with glutamic acid, leucine did not show activation when RH < 100% (Figure 7). This result was expected since leucine was not CCN active at supersaturation condition as shown in previous section. Again, there is no literature information to confirm this result. Hu et al. [2010] suggests that large particles are easier to uptake water because they contain more solute than smaller ones. This hypothesis could explain the difference between leucine and glutamic acid hygroscopic behaviors since as stated above, glutamic acid is a bigger molecule than leucine.

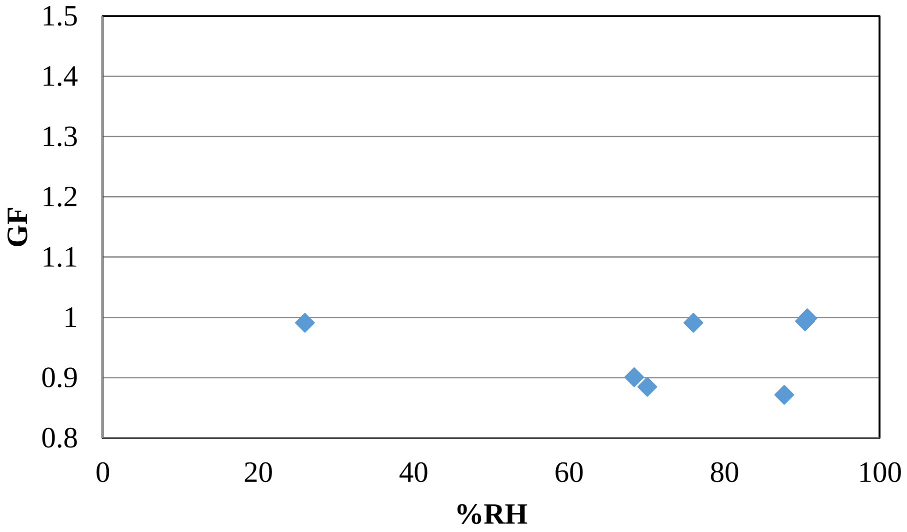

Figure 7. GF as a function of % relative humidity of leucine (80nm)

4. *Kappa Parameter:*

By plotting experimentally-determined critical SS as a function of dry particle diameters against known constant κ lines calculated from Petters and Kreidenweis' equation, we can establish the range of κ values for glutamic acid. As seen in Figure 8, glutamic acid κ ranges from 0.1 to 0.4 and the majority is between 0.2 and 0.3. This result is in good agreement with Petters and Kreidenweis' values which were calculated using Huff Hartz et al. [2006] and Raymond and Pandis [2003] data (Table 3). Additionally, the κ values of glutamic acid are in the expected range for organic species (0.01 to 0.5). These low values of κ indicate that glutamic acid is not as CCN active as some other inorganic species such as NaCl (κ =1.28) [Petters and Kreidenweis, 2007]. However, glutamic acid is still in the high range of CCN active for organic species.

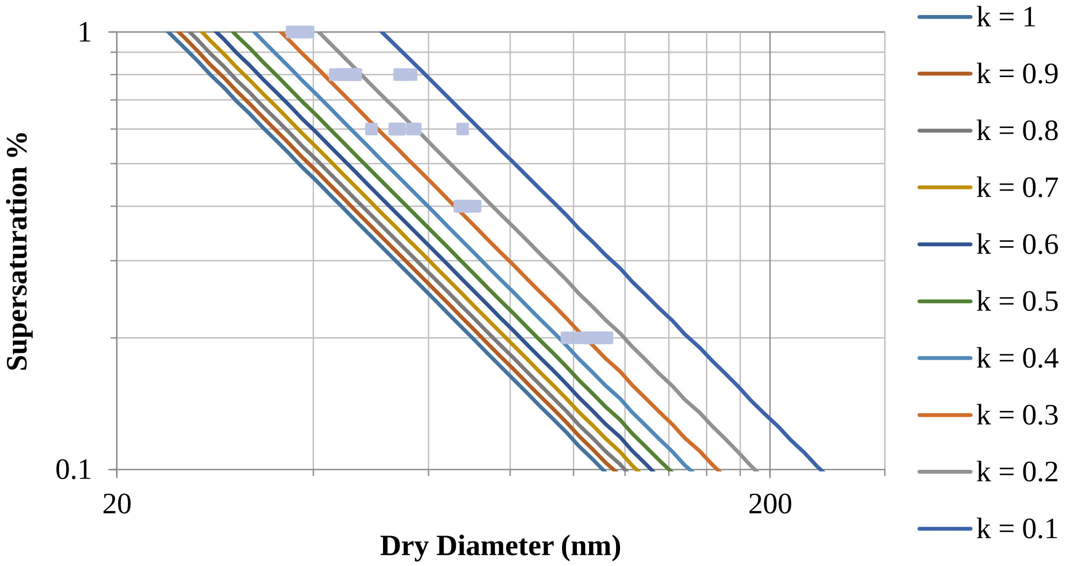

Figure 8. Constant Kappa's from 0.1 to 1 calculated from Petters and Kreidenweis' equation [2007]. The Markers are data derived from CCN activity of glutamic acid.

Values of κ were also calculated using Petters and Kreidenweis' equation using both data from SMCA and hygroscopic GF (Table 4). The results of κ derived from SMCA confirm the observation from Figure 8. Moreover, κ values derived from SMCA (0.17 – 0.53) are higher than κ values derived from hygroscopic GF (0.09 – 0.2). However, since κ values derived from SMCA have a wider range, κ values derived from GF are still within that range of values. Using Huff Hartz et al. [2006] data, the GF derived κ has a similar value with our mean value (0.14 vs 0.15). It is also noted that as %RH increases, κ value also increases. This trend was also observed in Ruehl et al. study [2010]. The result indicates that as more water introduces into the environment, κ value increases which mean the particles become more CCN active. In other words, once the particle is activated, its growth is only limited by the amount of water in the environment.

Table 4: κ values derived from CCN and hygroscopic GF of glutamic acid.

	This Study	**Petters and Kreidenweis [2007] using Huff Hartz et al.'s Data [2006]**	**Petters and Kreidenweis [2007] using Raymond and Pandis's Data [2003]**
CCN Derived κ	0.17 – 0.53 0.35 (Mean)	0.11 – 0.32 0.18 (Mean)	0.16 – 0.42 0.25 (Mean)
GF Derived κ	0.09 – 0.20 0.14 (Mean)	0.15	N/A

Figure 9 summarizes and compares the results of κ values derived from SMCA and hygroscopic GF from this study as well as κ values calculated using water properties. Again, the

CCN derived κ values are close to κ values calculated using water properties. This confirms the conclusion drawn from CCN activity analysis that surface tension does not have a significant impact on the prediction of CCN activity of compounds. Additionally, those results are higher than κ values derived from hygroscopic GF (orange markers).

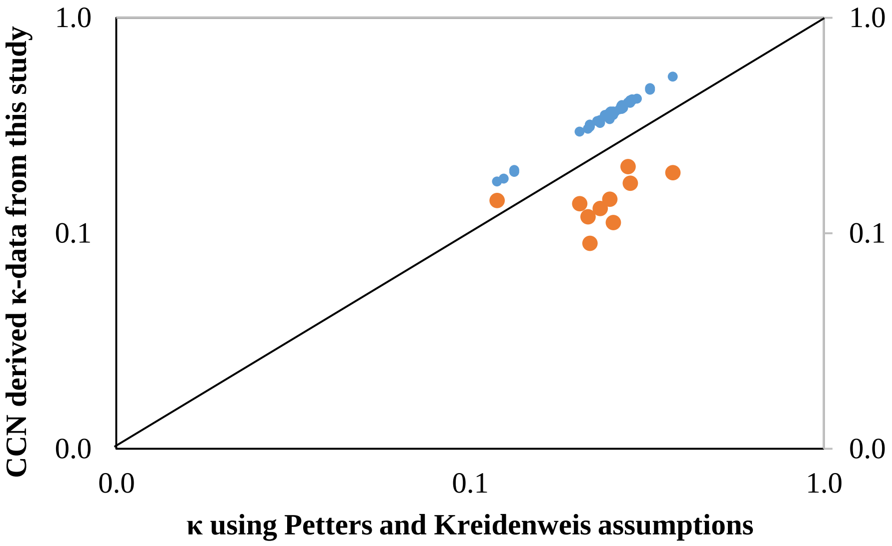

Figure 9. Comparison of κ values derived from different techniques (CCN and GF) as well as values calculated using water assumption. Orange markers are GF derived κ values.

5. *SEM Images:*

A droplet generator was used to generate micron sized particles which were collected on a steel disk. The particles were then viewed under a scanning electron microscope (SEM) to determine the size and morphology. Images were captured and recorded for both leucine and glutamic acid (Figure 10 and 11 respectively). As seen in the images, the particles are uniform and have diameters of approximately 20 µm. Moreover, both leucine and glutamic acid particles have a fairly sphere shape. Glutamic acid particles have a spike or needle-like surface (Figure 10) while leucine particles have a smooth surface (Figure 11).

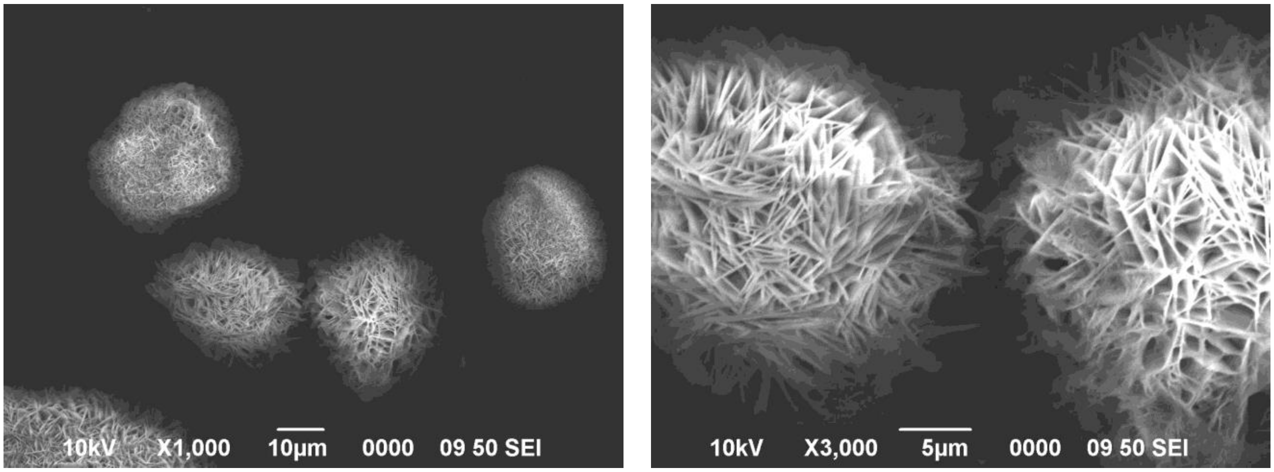

Figure 10. Glutamic acid particles prepared from water SEM images

Glutamic acid morphology suggests that the nucleation happens in the center of particles. Due to the symmetry of the molecule and the fact that glutamic acid is fairly hydrophilic, it is well mixed with water. When water evaporates, the solute concentrates more in the center of the particles leaving the water at the edge of the particles. When more water evaporates, the particles crystallize around the center and leave the shape as seen in Figure 10.

On the other hand, leucine morphology suggests that the nucleation process happens on the surface of particles. As seen in Figure 11, leucine has a cap shaped particle and the particle is hollow. Leucine is not as symmetrical and hydrophilic as glutamic acid (only one carboxylic acid group), it does not mix well with water and has a preference of alignment with water molecules. The hydrophilic part of leucine molecule likes to be in the inside with water while the carbon side of the molecule likes to face the edge of the particle. Therefore, even before water evaporates, the solute already concentrates more around the boundary of the particle. The water is now trapped inside and the particle collapses in when the nucleation proceeds (Figure 11).

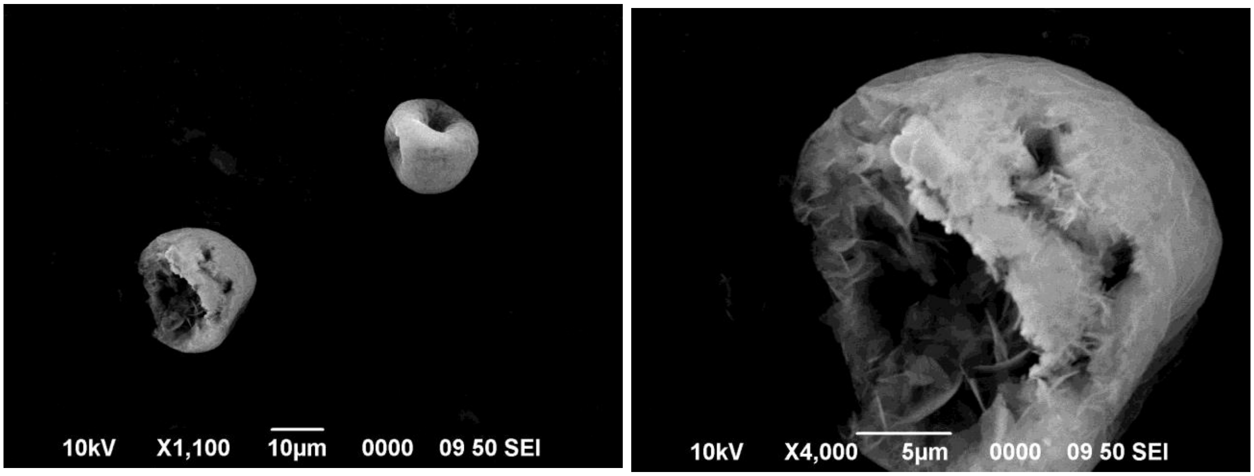

Figure 11. Leucine particles prepared from water SEM images

6. *AFM images*

Both compounds were generated under a simple impactor to collect nano-size particles on a mica disc. The samples were then viewed under the Atomic Force Microscopy (AFM) and the resulting images were analyzed using the Gwyddion software. Figure 12 shows the overview images of glutamic acid (to the left) and leucine (to the right). The images indicate that glutamic acid particles have a larger diameter (~0.6 μm) compared with leucine (~1/3 μm). It was suspected that the glutamic acid particles were still wet when they landed on the sample plate and the leucine particles had been crystallized. Morover, leucine particles are as tall as 140 nm while glutamic acid particles heights are around 60 nm.

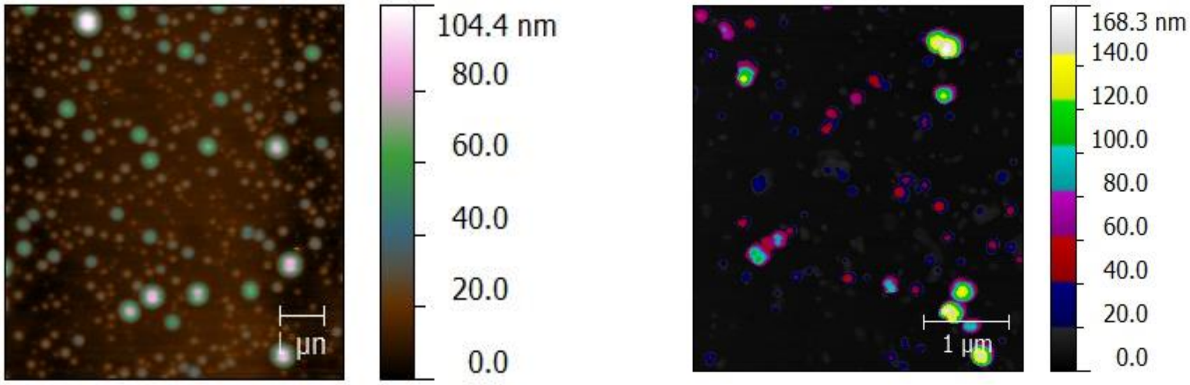

Figure 12. AFM images of glutamic acid (left) and leucine (right)

When taking a close look to glutamic acid particles, both the profile graph (Figure 13) and the 3D image (Figure 14) show that glutamic acid particles have a smooth and identical surface. On the other hand, leucine's profile graph and 3D image confirm that it has an uneven surface (Figure 15 and 16 respectively). In fact, the AFM 3D images show that leucine particles have a cap shape similar to what the SEM images show.

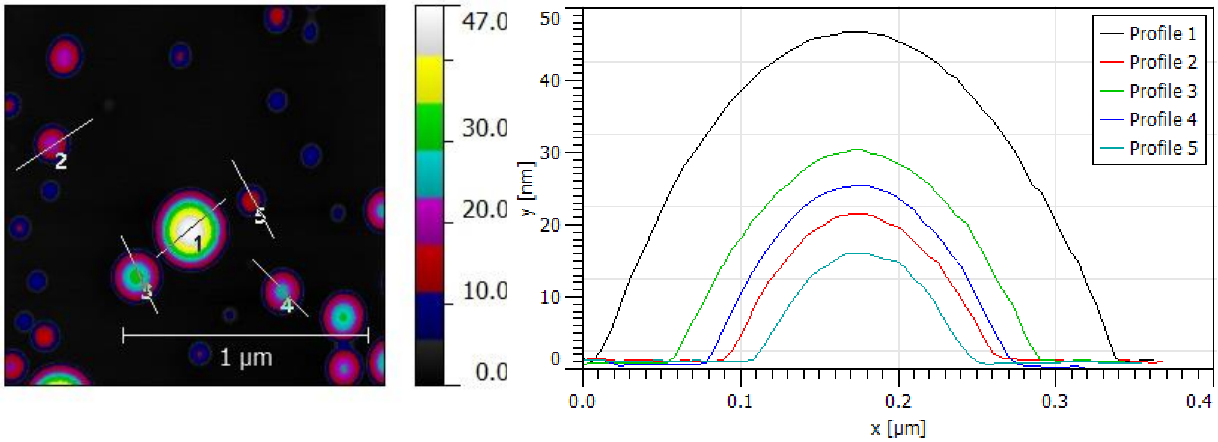

Figure 13. Profile graphs of selected glutamic acid particles

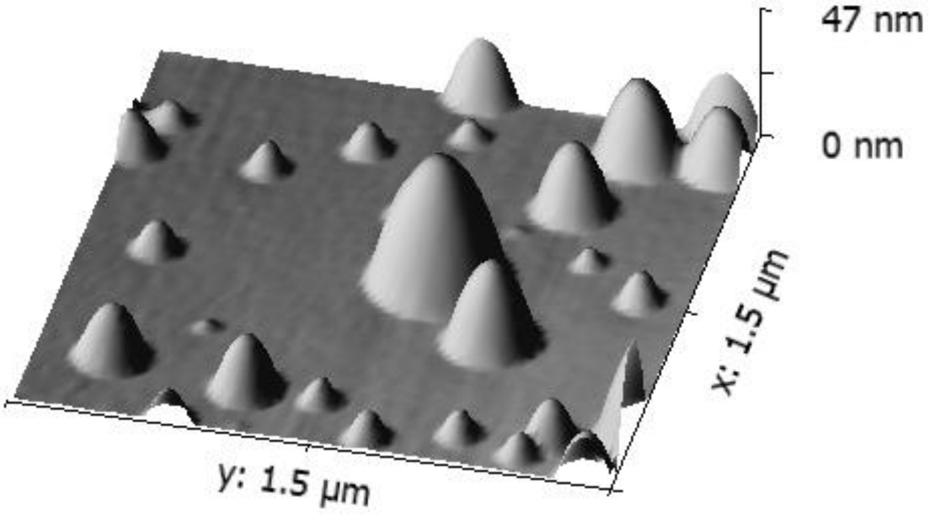

Figure 14. 3D image of glutamic acid particles

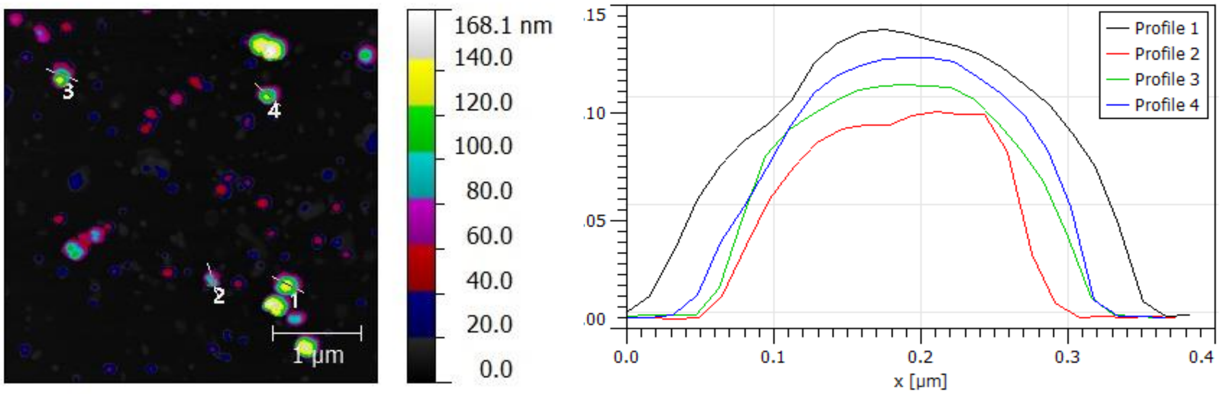

Figure 15. Profile graph of selected leucine particles

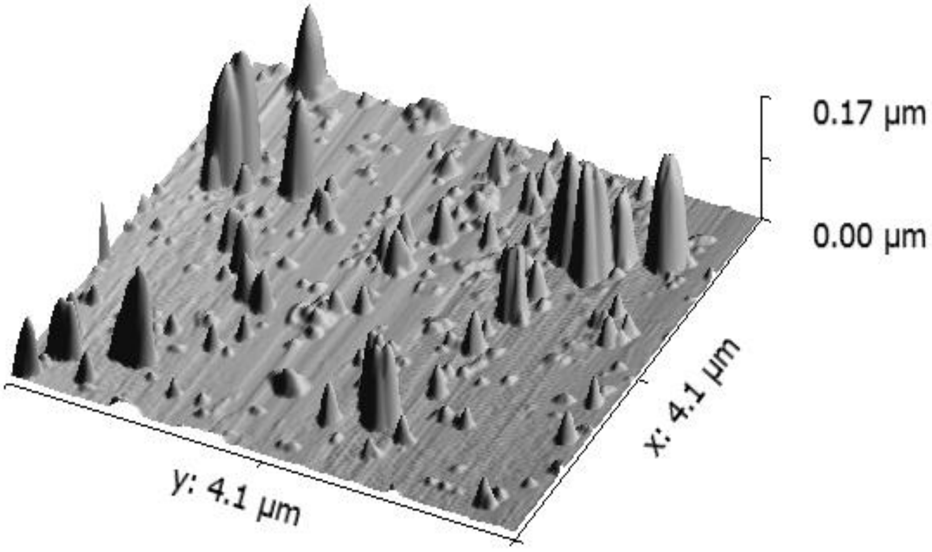

Figure 16. 3D image of leucine particles

Conclusions

Two organic aerosol species, leucine and glutamic acid, were investigated for various aspects using different techniques including SMPS, CCNC, H-TDMA, SEM and AFM. Various properties of those species include solubility, surface tension, water interactions and particles morphology. Leucine has a higher solubility than glutamic acid (18.7 g/L and 7.2 g/L solubility respectively). However, glutamic acid has a slightly higher surface tension than leucine (83.8 mN/m and 80.2 mN/m respectively). Activation diameters were experimentally measured at various supersaturation conditions (0.2 to 1%). Leucine did not show any CCN activity at the condition that we studied. Dry particle diameters range from 37 nm to 113 nm for glutamic acid. Köhler theory with different assumptions was also applied to verify the experimental results. Overall, the theoretical results are in good agreement with the experimental results regardless of which surface tension was used. Additionally, hygroscopic behavior of leucine and glutamic acid was also studied. Again, leucine particles did not show activation at RH < 100%. Glutamic acid particles activate at 83.3% RH and grow into droplets as big as 1.4 times the initial particle. Moreover, the κ values were also computed for glutamic acid using both CCN data and hygroscopic GFs. Values of κ ranged from 0.17 to 0.53 and 0.09 to 0.2 using CCN data and GFs respectively. Finally, the SEM and AFM images of glutamic acid suggest that the particles are smooth and crystallized from the center. On the other hand, SEM and AFM images of leucine show that the nucleation process takes place on the boundary of the particles and the particles surface is uneven. Various results of this study were contradicted with what was expected and cannot be explained by chemistry theory; therefore, further investigation will be necessary.

References

Aalto, P., Kulmala, M., 2000. Using a cloud condensation nuclei counter to study CCN properties and concentrations. Boreal Environment Research 5, 349-359.

Acker, K., Mertes, S., Moller, D., Wieprecht, W., Auel, R., Kalasz, D., 2002. Case study of cloud physical and chemical processes in low clouds at Mt. Brocken. Atmospheric Research 64, 41-51.

Ambwani, D. S., and T.Fort Jr., 1979. Surface and Colloid Science. Plenum, New York.

Andrew, E., Kreidenweis, S. M., Penner, J. E., Larson, S. M., 1997. Potential origin of organic cloud condensation nuclei observed at marine site. Journal Geophysical Research 102, 21,997-22,012.

Artaxo, P., Hansson, H.-C., 1995. Size distribution of biogenic aerosol particles from the Amazon Basin. Atmospheric Environment 29, 393-402.

Biskos, G., Russell, L. M., Buseck, P. R., Martin, S. T., 2006. Nanosize effect on the hygroscopic growth factor of aerosol particles. Aerosol Science and Technology 40 (2), 97-106.

Castro, M.S., Driscoll, C.T., Jordan, T.E., Reay, W.G., Boynton, W.R., Seitzinger, S.P., Styles, R.V., Cable, J,E., 2001. Contribution of atmospheric deposition to the total nitrogen loads to thirty-four estuaries on the Atlantic and Gulf coasts of the United States. In: Nitrogen loading in coastal water bodies: an atmospheric perspective. AGU, 77–106.

Chan, M.N., Choi, M.Y., Ng, N.L., Chan, C.K., 2005. Hygroscopicity of water-soluble organic compounds in atmospheric aerosols: amino acids and biomass burning derived organic species. Environmental Science Technology 39(6), 1555–1562.

Corrigan, C.E., Novakov, T., 1999. Cloud condensation nucleus activity of organic compounds: a laboratory study. Atmospheric Environment 33, 2661-2668.

Cruz, C.N., Pandis, S.N., 1997. A study of the ability of pure secondary organic aerosol to act as cloud condensation nuclei. Atmospheric Environment 31 (15), 2205-2214.

Cruz, C.N., Pandis, S.N., 2000. Deliquescence and hygroscopic growth of mixed inorganic – organic atmospheric aerosol. Environmental Science Technology 34, 4313-4319.

de Haan, D.O.D., Corrigan, A.L., Smith, K.W., Stroik, D.R., Turley, J.J., Lee, F.E., Tolbert, M.A., Jimenez, J.L., Cordova, K.E., Ferrell, G.R., 2009. Secondary organic aerosol-forming reactions of glyoxal with amino acids. Environmental Science Technology 43(8), 2818–2824.

Dennis, R., Haeuber, R., Blett, T., Cosby, J., Driscoll, C., Sickles, J., Johnston, J., 2007. Sulfur and nitrogen deposition on ecosystems in the United States. EM-PITTSBURGH-AIR AND WASTE MANAGEMENT ASSOCIATION, 12.

Eichel, C., Krämer, M., Schütz, Wurzler S., 1996. The solubility of atmospheric aerosol particles and its impact on cloud microphysics. Journal Aerosol Science 27, s81-s82.

Facchini, M. C., Decesari, S., Mircea, M., Fuzzi, S., Loglio, G., 2000. Surface tension of atmospheric wet aerosol and cloud/fog droplets in relation to their organic carbon content and chemical composition. Atmospheric Environment 34, 4853-4857.

Ge, X., Wexler, A.S., Clegg, S.L., 2010. Atmospheric amines-part I. A review. Atmospheric Environment.

Gorbunov, B., Hamilton, R., 1997. Water nucleation on aerosol particles containing both soluble and insoluble substances. Journal Aerosol Science 28, 239-248.

Gysel, M., Weingartner, E., Baltensperger, U., 2002. Hygroscopicity of aerosols particles at low temperatures. 2. Theoretical and experimental hygroscopic properties of laboratory generated aerosols. Environmental Science Technology 36, 63-68.

Hartmann D.L. & Doelling D., 1991. On the net radiative effectiveness of clouds. Journal of Geophysical Research 96, 869-891.

Hu, D., Qiao, L., Chen, J., Ye, X., Yang, X., Cheng, T., Fang, W., 2010. Hygroscopicity of inorganic aerosols: size and relative humidity effects on the growth factor. Aerosol and Air Quality Research 10, 255-264.

Hudson, J. G., Da, X., 1995. Volatility and size of cloud condensation nuclei. Journal of Geophysical Resarch 101, 4435-4442.

Hori, M., Ohta, S., Murao, N., Yamagata, S., 2003. Activation capability of water soluble organic substances as CCN. Journal of Aerosol Science 34, 419-448.

Huff-Hartz, K. E. H., Tischuk, J. E., Chan, M. N., Chan C. K., Donahue, N. M., Pandis, S. N., 2006. Cloud condensation nuclei activation of limited solubility organic aerosol. Atmospheric Environment 40 (4), 605-617.

Intergovernmental Panel on Climate Change, 1995. Climate Change 1994: Radiative Forcing of Climate. Cambridge University Press, New York.

Jacobson, M.C., Hansson, H.-C., Noone, K.J., Charlson, R.J., 2000. Organic atmospheric aerosols: review and state of the science. Reviews of Geophysics 38, 267-294.

Jin, X. Z., Chao, K. C., 1992. Solubility of four amino acids in water and of four pairs of amino acids in their water solutions. Journal of Chemical and Engineering Data 37 (2), 199-203.

Köhler, H., 1936. The nucleus in and the growth of hygroscopic droplets. Trans. Faraday Society 32, 1152-1161.

Knutson, E. O., Whitby, K. T., 1975. Aerosol classification by electrical mobility: apparatus, theory, and applications. Journal of Aerosol Science 6, 443-451.

Kristensson, A., Rosenorn, T., Bilde, M., 2010. Cloud droplet activation of amino acid aerosol particles. Journal of Physics Chemistry A. 114, 379-386.

Kumala, M., Laaksonen, A., Charlson, R.J., Korhonen, P., 1997. Cloud without supersaturation. Nature 388, 336-337.

Kumar, P.P, Broekhuizen, K., Abbatt, J.P.D., 2003. Organic acids as cloud condensation nuclei: laboratory studies of highly soluble and insoluble species. Atmospheric Chemistry and Physics 3, 509-520.

Kuznetsova, M., Lee, C., Aller, J., 2005. Characterization of the proteinaceous matter in marine aerosols. Mar Chem 96(3–4), 359–377.

Laaksonen, A., Korhonen, P., Kulmala, M., Charlson, R.J., 1998. Modification of the Köhler equation to include soluble trace gases and slightly soluble substances. Journal of Atmospheric Science 55, 853-862.

Laskin, A., Smith, J.S., Laskin, J., 2009. Molecular characterization of nitrogen-containing organic compounds in biomass burning aerosols using high-resolution mass spectrometry. Environmental Science Technology 43(10), 3764–3.

Liu, B. Y. H., Pui, D. Y. H., 1974. A submicron aerosol standard and the primary, absolute calibration of the condensation nuclei counter. Journal Colloid Interface Science 47, 155-171.

Mace, K.A., Artaxo, P., Duce, R.A., 2003. Water-soluble organic nitrogen in Amazon Basin aerosols during the dry (biomass burning) and wet seasons. Journal of Geophysical Research 108 (D16), 4512.

Mace, K.A., Duce, R.A., Tindale, N.W., 2003. Organic nitrogen in rain and aerosol at Cape Grim, Tasmania, Australia. Journal of Geophysical Research 108 (D11), 4338.

Mace, K.A., Kubilay, N., Duce, R.A., 2003. Organic nitrogen in rain and aerosol in the eastern Mediterranean atmosphere: an association with atmospheric dust. Journal of Geophysical Research 108 (D10), 4320.

Masclet, P., Hoyau, V., 1995. Speciation of particulate organic matter in arctic aerosols. Journal Aerosol Science 26, s473.

Matsumoto, K., Tanaka, H., Nagao, I., Ishizaka, Y., 1997. Contribution of particulate sulfate and organic carbon to cloud condensation nuclei in the marine atmosphere. Geophysical research Letters 24, 655-658.

Matsumoto, K., Uematsu, M., 2005. Free amino acids in marine aerosols over the western North Pacific Ocean. Atmospheric Environment 39 (11), 2163-2170.

Milne, P.J., Zika, R.G., 1993. Amino acid nitrogen in atmospheric aerosols: occurrence, sources and photochemical modification. Journal of Atmospheric Chemistry 16(4), 361–398.

Moore, H. R., Nenes, A., Medina, J., 2010. Scanning mobility CCN analysis – A method for fast measurements of size-resolved CCN distributions and activation kinetics. Aerosol Science and Technology, 44(10), 861-871.

Mopper, K., Zika, R.G., 1987. Free amino acids in marine rains: evidence for oxidation and potential role in nitrogen cycling. Nature 325(6101), 246–249.

Novakov, T., Penner, J.E., 1993. Large contributions of organic aerosols to cloud-condensation nuclei concentrations. Nature 365, 823-825.

Posfai, M., Xu, H., Anderson, J. R., Buseck, P. R., 1998. Wet and dry sizes of atmospheric aerosol particles: an AFM-TEM study. Geophysical Research Letters, 25 (11), 1907-1910.

Petters, M. D., Kreidenweis, S. M., 2007. A single parameter representation of hygroscopic growth and cloud condensation nucleus activity. Atmospheric Chemistry and Physics 7, 1961-1971.

Pruppacher, H. R., and Klett, J. D., 1980. Microphysics of clouds and precipitation. D. Reidel, Norwell, Mass.

Raymond, T.M., Pandis, S.N., 2002. Cloud activation of single-component organic aerosol. Journal of Geophysical Research 107 (D24), 4787.

Ruehl, C. R., Chuang, P. Y., Nenes, A., 2010. Aerosol hygroscopicity at high (99 to 100%) relative humidities. Atmospheric Chemistry and Physics 10, 1329-1344.

Sattler, B., Puxbaum, H., Psenner, R., 2001. Bacterial growth in supercooled cloud droplets. Geophysical Research Letter 28(2), 239–242.

Saxena, P., Hildemann, L. M., 1996.Water-soluble organics in atmospheric particles: A critical review of the literature and application of thermodynamic to identify candidate compounds. Journal Atmospheric Chemistry 24, 57-109.

Scheller, E., 2001. Amino acids in dew-origin and seasonal variation. Atmospheric Environment 35(12), 2179–2192.

Seinfeld J.H. & Pandis S.N., 1998. Atmospheric chemistry and physics: from air pollution to climate change. A Wiley-Interscience publication, USA, pp.1326.

Shulman, M.L., Jacobson, M.C., Charlson, R.J., Synovec, R.E., Young, T.E., 1996. Dissolution behavior and surface tension effects of organic compounds in nucleating cloud droplets. Geophysical Research Letters 23, 277-280.

Sun, J., Ariya, P.A., 2006. Atmospheric organic and bio-aerosols as cloud condensation nuclei (CCN): A review. Atmospheric Environment 40, 795-820.

Tong, Y., Lighthart, B., 2000. The annual bacterial particle concentration and size distribution in the ambient atmosphere in a rural area of the Willamette Valley, Oregon. Aerosol Science and Technology 32(5), 393–403.

Twomey S., 1977. The influence of pollution on the shortwave albedo of clouds. Journal of Atmosphere Science 34, 1149-1152.

Wedyan, M.A., Preston, M.R., 2008. The coupling of surface seawater organic nitrogen and the marine aerosol as inferred from enantiomer-specific amino acid analysis. Atmospheric Environment 42, 8698-8705.

Wiedensohler, A., 1988. An approximation of the bipolar charge distribution for particles in the submicron size range. Journal Aerosol Science 19, 387-389.

Wouters, L., Hagedoren, S., Dierck, I., Artaxo, P., Grieken, R.V., 1993. Laser microprobe mass analysis of Amason Basin aerosols. Atmospheric Environment 27, 661-668.

Xiong, J. Q., Zhong, M., Fang, C., Chen, L. C., Lippmann, M., 1998. Influence of organic films on the hygroscopicity of ultrafine sulfuric acid aerosol. Environmental Science and Technology 32 (22), 3536-3541.

Yu, Z., Zhang, Q., Kraus, T., Dahlgren, R., Anastasio, C., Zasoski, R., 2002. Contribution of amino compounds to dissolved organic nitrogen in forest soils. Biogeochemistry 61(2), 173–198.

Zhang, Q., Anastasio, C., Jimenez-Cruz, M., 2002. Water-soluble organic nitrogen in atmospheric fine particles (PM2. 5) from northern California. Journal of Geophysical Research 107, 4112.